A Novel Synchronous Rotating Frame Transformation for Complete Synchronous Vibration Force Suppression

Qian Zhou [a], Cong Peng [a], Mengting Zhu, Zhiquan Deng

[a] Nanjing University of Aeronautics and Astronautics, No.29 Jiangjun Road, 211100 Nanjing, China, pengcong@nuaa.edu.cn

Abstract—**Unbalance vibration force is critical in normal operation of magnetic bearings. Among all vibration forces, the synchronous vibration force is the most influential factor. To effectively suppress the unbalance force caused by the mass unbalance of high-speed magnetic suspend rotor, in this work, a novel method for active magnetic bearings based on the synchronous rotating frame (SRF) transformation is adopted. In this case, the magnetic bearing force is directly set as the input of the SRF transformation. The structure and principle of SRF transformation is proposed. In order to maintain the system stability, stability analysis which is related to the SRF transformation is conducted. In order to ensure the stability of the whole close-loop system, only one parameter needs to adjust. Simulation results show that the proposed method can effectively suppress synchronous vibration force. Compared with the conventional method of vibration force suppression the method proposed has batter performance.**

I. Introduction

As is a non-contact support structure, Active magnetic bearings (AMBs) have many promising and practical advantage over conventional mechanical bearings, such as lower rotating frictional loss, lubrication elimination, higher rotational speed and adjustable stiffness. With so many advantages, magnetic suspended bearings are widely used in high speed motors, molecular pumps and spacecraft attitude control [1]. Despite of the advantages, unbalance mass, caused by the limitation of machining accuracy as well as the principle of geometry axis is not coincident with its inertial axis. Unbalance mass with small amplitude can lead to serious vibration [8]. When the rotor rotates at a very high speed, the vibration turned even more severe because of the centrifugal force which is proportional to the square of the rotation speed. Unbalance vibration force transferred to the outside through the casing can generate noise, vibration even damage of mechanical equipment. Hence, it is necessary to adopt active control method to suppress synchronous vibration force.

There have many previous research works on vibration suppression of the magnetic suspended rotor control system. There are two main control strategies for real time vibration force suppression. One is to set the position of the inertial axis as the control target, then force the rotor to rotate around the inertial axis. This approach can suppress vibration force, but this approach needs to identify the inertial axis position which relative to the reference frame.The effect of suppression mainly depends on the identification precision of inertial axis. When the unbalance is small, the sensor installation and detection error can weaken the vibration suppression effect. Another approach is to directly set the synchronous vibration force or torque as the target, then eliminate it by proposed control algorithm. This method can eliminate the synchronous component in control current and displacement. In [4] a method based on (Least Mean Square, LMS) was proposed to compensate synchronous current by feed forward signals synchronous to current with the same amplitude. Another repetitive learning algorithm in [5] was proposed to adjust learning rate adaptively, which can suppress synchronous current in large speed range. However, these methods did not take the vibration caused by displacement stiffness force into consideration.

In this paper, an improved synchronous vibration force suppression algorithm based on SRF is proposed. We set the vibration force as the input of SRF directly, then feedback the output of SRF to the current loop of origin system, which construct a novel notch filter. SRF transformation can track the harmonic signals of a certain frequency and can apply real-time compensation. SRF has been applied in three phase induction motors but seldom applied in the vibration suppression of AMBs [2]-[3]. To the best knowledge, there is no literature in which this method has been used to suppress synchronous vibration force in magnetic bearings control system.

The main idea is that: 1) After the SRF transformation, the harmonic and fundamental components of synchronous vector can be decomposed easily; 2) Harmonic components can be eliminated through a low-pass filter; 3) Adjust only one parameter can ensure the global stability. Then stability analysis is provided and synchronous vibration force is suppressed effectively.

The rest of paper is arranged as follows. In section Ⅱ, a model of magnetic suspended rotor with mass unbalance is build. In section Ⅲ, the principle of SRF is proposed and in section Ⅳ, stability analysis of the close-loop is given. Simulation results are presented in section Ⅴ. Finally, conclusions are provided in SectionⅥ.

II. Dynamic Modeling with Mass Unbalance

The structure of rotor with unbalanced mass is shown in the Fig. 1. The existence of the static imbalance and dynamic imbalance of rotor resulting from that geometry center and the mass center do not coincide. The principle axis of inertia is not coincident with its axis of geometry. In this paper, only motions in four radial DOFs are investigated, for the reason that unbalance effect exist in the radial direction. The diagram

This work is supported by National Nature Science Foundation under Grant 61703203 and 51577087, Nature Science Foundation of Jiangsu Province under Grant BK 20170812

of radial magnetically suspended rotor with mass unbalance is showing in Fig1.

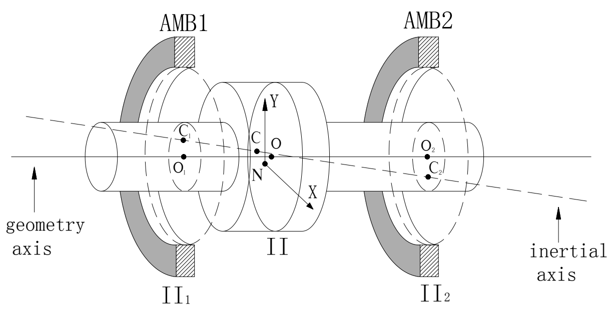

Figure 1. The basic structure diagram of magnetic suspended rotor with mass unbalance .

Let Π_1 and Π_2 represent the central plane of magnetic bearing A and B respectively. Π is the central plane of the rotor. C_1、C_2、C represent the intersection point between the inertial axis and plane Π_1、Π_2、Π respectively and O_1、O_2、O represent the intersection point between the geometric axis and plane Π_1、Π_2、Π . Then N represent the point of intersection between the central line of two AMBs and plane Π . N donate the origin of the stationary frame NXY and O is the origin of the rotating frame $O\varepsilon\eta$ in the central plane of rotor. The rotating frame rotates at the speed of rotator- Ω . loc is the distance vector between the rotator mass center and geometric center. lo_1c_1 and lo_2c_2 are the distance vector form O_1 to C_1 and O_2 to C_2 respectively. θ is the angle between OC and $O\varepsilon$. ξ is the distance of OC . Φ, θ are the angle between $O\varepsilon$ and the projection of lo_1c_1 and lo_2c_2 in plane Π . (X_A, Y_A) 、 (X_B, Y_B) 、 (X_A, Y_A) 、 (X_B, Y_B) are defined as coordinates of O_1 、 O_2 、 C_1 、 C_2 in stationary frame NXY respectively. The coordinate can be expressed as

$$\begin{cases} X_A(t) = x_A(t) + \psi_{AX}(t) \\ Y_A(t) = y_A(t) + \psi_{AY}(t) \\ X_B(t) = x_B(t) + \psi_{BX}(t) \\ Y_B(t) = y_B(t) + \psi_{BY}(t) \end{cases} \quad (1)$$

where $\psi_{AX}(t)$、$\psi_{AY}(t)$、$\psi_{BX}(t)$、$\psi_{BY}(t)$ can be described as

$$\begin{cases} \psi_{AX}(t) = l\cos(\Omega t + \theta) - m\cos(\Omega t + \alpha) \\ \psi_{AY}(t) = l\sin(\Omega t + \theta) + m\sin(\Omega t + \alpha) \\ \psi_{BX}(t) = l\cos(\Omega t + \theta) + n\cos(\Omega t + \beta) \\ \psi_{BY}(t) = l\sin(\Omega t + \theta) - n\sin(\Omega t + \beta) \end{cases} \quad (2)$$

When the rotor moves in a small area near the equilibrium position, the equation of magnetic force can be linearized as

$$\begin{cases} F_{AX} = k_s X_A + k_i i_{AX}(X_A) \\ F_{AY} = k_s Y_A + k_i i_{AY}(Y_A) \\ F_{BX} = k_s X_B + k_i i_{BX}(X_B) \\ F_{BY} = k_s Y_B + k_i i_{BY}(Y_B) \end{cases} \quad (3)$$

where F_{AX}、F_{AY}、F_{BX} and F_{BY} are the magnetic forces generated by bearings A and B in x and y directions, respectively. i_{AX}、i_{AY}、i_{BX}、i_{BY} are control current for bearings A and B in x and y directions, respectively. k_i and k_s donate the current stiffness and displacement stiffness of AMB, respectively. Let

$$\begin{cases} \psi_{AX}(t) = -\xi\cos(\Omega t + \varphi) \\ \psi_{AY}(t) = -\xi\sin(\Omega t + \varphi) \\ \psi_{BX}(t) = -\xi\cos(\Omega t + \varphi) \\ \psi_{BY}(t) = -\xi\sin(\Omega t + \varphi) \end{cases} \quad (4)$$

then the equation of magnetic forces with mass unbalance can be derived as

$$\begin{cases} F_{AX} = k_s(X_A + \psi_{AX}) + k_i(i_{AX}(x_A + \psi_{AX})) \\ F_{AY} = k_s(Y_A + \psi_{AY}) + k_i(i_{AY}(y_A + \psi_{AY})) \\ F_{BX} = k_s(X_B + \psi_{BX}) + k_i(i_{BX}(x_B + \psi_{BX})) \\ F_{BY} = k_s(Y_B + \psi_{BY}) + k_i(i_{BY}(y_B + \psi_{BY})) \end{cases} \quad (5)$$

where ψ_{AX}、ψ_{AX}、ψ_{AX}、ψ_{AX} are displacement disturbance in A 、 B bearings generated by mass unbalance, respectively. According to equation (5), both displacement component and current component of magnetic forces containing unbalance disturbances.

III. The Principle of SRF Transformation

To simplify the algorithm description, two coordinate systems are defined, C and M represent the mass center and geometric center of the rotor, respectively. Set C as the origin of the static reference frame CX_sY_s and Set M as the origin of the bearing-rotor coordinate CX_rY_r which rotate with the speed of Ω . It can be derived that the motion trajectory of the geometric center M with the mass center C is a circle. Therefore the displacement coordinate of geometric center M in rotating frame is a constant vector.

Let $[X_s, Y_s]$ and $[X_r, Y_r]$ represent the motion coordinate of M in static reference frame and rotating frame, respectively. Then it can be derived that

$$\begin{bmatrix} X_r \\ Y_r \end{bmatrix} = T(\Omega t)\begin{bmatrix} X_s \\ Y_s \end{bmatrix} \quad (6)$$

where

$$T(\Omega t) = \begin{pmatrix} \cos(\Omega t + \theta) & \sin(\Omega t + \theta) \\ -\sin(\Omega t + \theta) & \cos(\Omega t + \theta) \end{pmatrix} \quad (7)$$

where $T(\Omega t)$ donate the SRF Transformation. Ω is the rotation speed of the rotor. θ represents the compensation angle for phase which is used to ensure the stability of the whole control system.

If the rotor rotates at a constant speed Ω, after the SRF transportation, the spectral characteristics of input signal is a dc component with mixed harmonic signal. Then the fundamental component can be extract by a low-pass filter. Although higher-order filters can improve the filtering effect, they will increase the calculation burden. Therefore, first-order filters are commonly employed, i.e.

$$g_f(s)=\frac{k}{s+\varepsilon} \tag{8}$$

At last, by applying a inverse SRF transportation and set the output of the first-order filters as the input of the inverse SRF transportation as follows, the synchronous vibration signal of the rotor can be reached.

$$\begin{pmatrix} X_c \\ Y_c \end{pmatrix} = T_{inv}(\Omega t)\begin{pmatrix} \hat{X}_r \\ \hat{Y}_r \end{pmatrix} \tag{9}$$

where $\hat{X}_r$, $\hat{Y}_r$ are outputs of first-order filters X_c, Y_c are synchronous vibration signal of the rotor, and $T_{inv}(\Omega t)$ is

$$T_{inv}(\Omega t)=\begin{pmatrix} \cos(\Omega t) & -\sin(\Omega t) \\ \sin(\Omega t) & \cos(\Omega t) \end{pmatrix} \tag{10}$$

The whole structure of the SRF transportation is shown in Fig2.

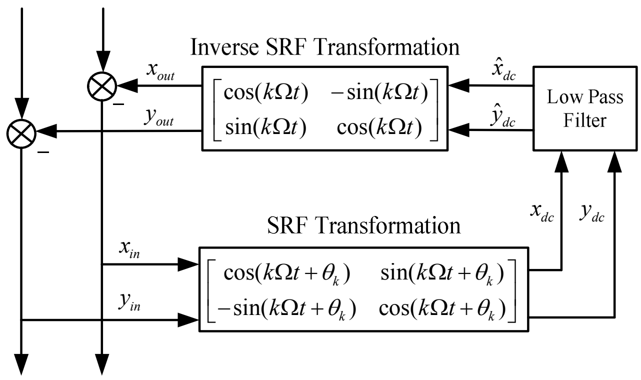

Figure 2. The general diagram of SRF transformation.

In this paper, the suppression of synchronous vibration force is mainly discussed. From equation (5). In order to eliminate the vibration force effectively, it is necessary to eliminate two parts force, which are synchronous current stiffness force and synchronous displacement stiffness force. Generally, the current stiffness and displacement stiffness are known constant values.

According to the location of the sensor, vibration signal in x and y axis have the same frequency but with phase difference of 90^o so complex variables were adopted, yields

$$X_{dc}(t)+jY_{dc}(t)=(X_{in}(t)+jY_{in}(t))e^{-j(\Omega t+\theta_k)} \tag{11}$$

The Laplace transform under zero initial conditions is deduced as

$$X_{dc}(s)+jY_{dc}(s)=(X_{in}(s-\Omega)+jY_{in}(s-\Omega))e^{-j\theta_k} \tag{12}$$

Typically, the transform function of low-pass filter is

$$G_f(s)=\frac{\varepsilon}{\lambda s+1} \tag{13}$$

Then it can be obtained that

$$\begin{aligned} \hat{X}_{out}(s)+j\hat{Y}_{out}(s) &= (\hat{X}_{dc}(s)+j\hat{Y}_{dc}(s))e^{j\Omega t} \\ &= \hat{X}_{dc}(s-j\Omega)+j\hat{Y}_{dc}(s-j\Omega) \\ &= (X_{in}(s)+jY_{in}(s))\frac{\varepsilon}{(\lambda s-j\Omega)+1}e^{-j\theta_k} \\ &= (X_{in}(s)+jY_{in}(s))G_k(s) \end{aligned} \tag{14}$$

Where $G_k(s)$ is the open-loop transfer function of SRF. Hence, the SRF close-loop transfer function can be derived as follows.

$$G_{fk}(s)=\frac{1}{1+G_k(s)}=\frac{(\lambda s-j\Omega)+1}{(\lambda s-j\Omega)+1+e^{-\theta_k j}\varepsilon} \tag{15}$$

The synchronous vibration force is directly set as the control target. The vibration force is constructed by synchronous current and displacement. Then set the synchronous vibration force as the input of the SRF. The structure of control system is shown in Fig3.

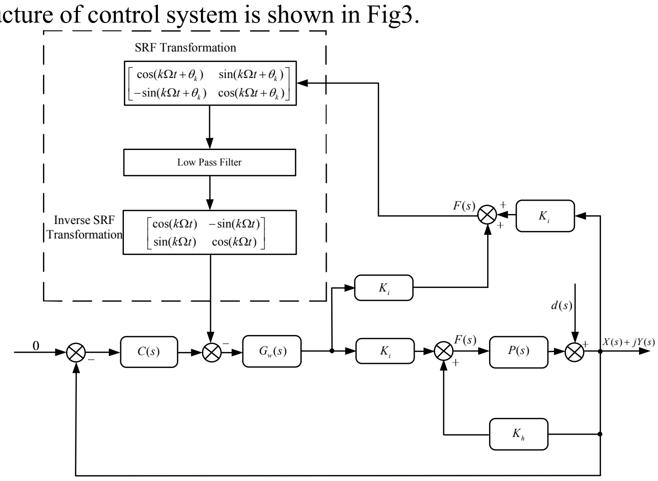

Figure 3. Close-loop control system of AMBs with SRF transformation

IV. STABILIYTY ANALYSIS

According to the system structure diagram, the characteristics polynomial of the close-loop transfer function can be obtained as

$$1+K_iG_c(s)G_w(s)P(s)-K_hP(s)+K_iG_{fk}(s)G_w(s)=0 \tag{16}$$

Substitute (15) into (16), then (16) can be written as follows

$$1+K_iG_c(s)G_w(s)P(s)-K_hP(s)+K_iG_{fk}(s)G_w(s)$$

$$=1+\frac{K_i(\frac{\lambda s-j\Omega+\varepsilon}{s-j\Omega+\varepsilon+ke^{-j\theta_k}})G_w(s)}{1+K_iG_c(s)G_w(s)P(s)-K_hP(s)} \tag{17}$$
$$=(\lambda s-j\Omega+\varepsilon+ke^{-j\theta_k})+\frac{K_i(\lambda s-j\Omega+\varepsilon)G_w(s)}{1+K_iG_c(s)G_w(s)P(s)-K_hP(s)}$$

As described in [6], a sensitivity function is used to prove stability. Set $S(s)$ as the sensitivity function of this control system.

$$S(s)=\frac{K_iG_w(s)}{1+K_iG_c(s)G_w(s)P(s)-K_hP(s)} \tag{18}$$

Assume that the system and $S(s)$ are stable before the SRF is added. Then the ploys of $S(s)$ remain in left complex plane. The (17) can be simplified as

$$(\lambda s-j\Omega+\varepsilon+ke^{-j\theta_k})+(\lambda s-j\Omega+\varepsilon)S(s)=0 \tag{19}$$

in which $k=\hat{k}K$, K is a constant value and $\hat{k}$ is a minimal value. (19) can be written as

$$\begin{aligned}\varsigma(s,\hat{k})&=(\lambda s-j\Omega+\varepsilon+\hat{k}Ke^{-j\theta_k})\\&+(\lambda s-j\Omega+\varepsilon)S(s)=0\end{aligned} \tag{20}$$

Only one ploy is obtained in characteristics polynomial, if $\hat{k}$ =0, which is

$$s=\frac{j\Omega-\theta_k}{\lambda} \tag{21}$$

After the insert of SRF transportation, ploys of close-loop system will lie within a small region of $s=(j\Omega-\theta)/\lambda$. According to (20) the derivative of s can be obtained when $\hat{k}$ =0 as follows

$$\frac{\partial s(k)}{\partial k}|_{k=0}=-\frac{\partial\varsigma(s,\hat{k})}{\partial k}/(\frac{\partial\varsigma(s,\hat{k})}{\partial s})=-\frac{Ke^{-j\theta_k}}{\lambda(1+S(j\Omega))} \tag{22}$$

In order to satisfy the stability requirements and ensure the motion of root locus to left after inserting the SRF, the real part of(22) need to less than zero as follows

$$\begin{cases}\mathrm{Re}\left[-\dfrac{Ke^{-j\theta_k}}{\lambda(1+S(j\Omega))}\right]<0\\[2ex]\mathrm{Im}\left[-\dfrac{Ke^{-j\theta_k}}{\lambda(1+S(j\Omega))}\right]=0\end{cases} \tag{23}$$

where Re[.] denote the real part and Im[.] means imaginary part. The stability condition shows in(23) is equal to the equation as follows

$$-\frac{\pi}{2}<\arg(\frac{Ke^{-j\theta_k}}{\lambda(1+S(j\Omega))})<\frac{\pi}{2} \tag{24}$$

For the sensitivity function $S(s)$, the Phase-frequency characteristic diagram is shown as Fig4, the Phase ranges from -90^o to 270^o , Theoretically, which dose not satisfied the stability requirements. So we can conclude from (24) that, with the change of rotor speed Ω , the system stability can be ensured by tuning the compensate angle θ_k .

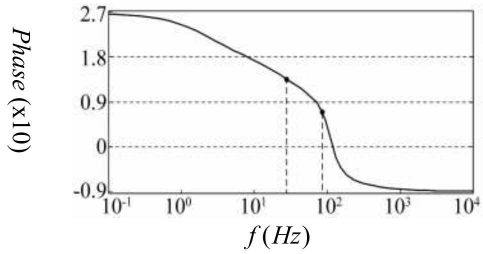

Figure 4. The phase frequency response curve of sensitivity function.

V. SIMULATION VERIFICATION

A. The verification of SRF based vibration suppression

In order to verify the effectiveness and feasibility of the direct vibration force suppression, control algorithm was carried out by an AMB model in Matlab/Simulink. Simulation parameters of AMB system are shown in Table1.

TABLE I. SIMULATION PARAMETERS

Parameter	Parameter	Value
m(kg)	rotor mass	4.08
k_p	Proportional coefficient	2.5
k_i	Integral coefficient	50
k_d	Differential coefficient	0.008
k_s (N/m)	Displacement stiffness	1.3×105
k_i (N/A)	Current stiffness	32
r_m	Distance	0.055m

Stability is the most important part of the entire control system. As mentioned previously, compensation angle θ plays a critical role for proposed method. To analyzed the close-loop system stability, The compensation angle was set as $\theta_k=0$, $\theta_k=\pi/2$,and $\theta_k=\pi$ according to different rotation speed.

Figs 5-7 illustrate the simulation result of the AMB system, when the rotor rotates at a speed of 50Hz(3000rpm) 、100Hz(6000 rpm) and 200Hz(12000rpm), respectively. It can be obviously derived form Fig5. and Fig6. that when the rotation speed is relatively low, such as 50Hz , and with the compensation angle $\theta_k=0$, the close-loop control system is out of stable. As shown in Fig. 5 (b), By Tuning the compensation angle θ_k to a proper value, the stability of the system is guaranteed. With the speed increasing, as shown in Fig. 6, the rotor speed is 100Hz and without compensation angle, the system is divergent. By adjusting compensation angle to $\theta_k=\pi/2$, then the proposed vibration suppression method performed well. When the rotation speed is high, the system become more stable. As shown in Fig. 7, the speed of rotor is 200Hz and $\theta_k=0$, the system is of convergence. On the contrary, with speed is 200Hz and $\theta_k\neq0$, the system become unstable. The simulation result provided an evidence for system stability that the proposed method for vibration force suppression has a negative effect on the stability of the close-loop system at low rotating speed. In [7] we can find the similar conclusion. After analysis, the divergence output of low-pass filter is the main cause for the system unstable.

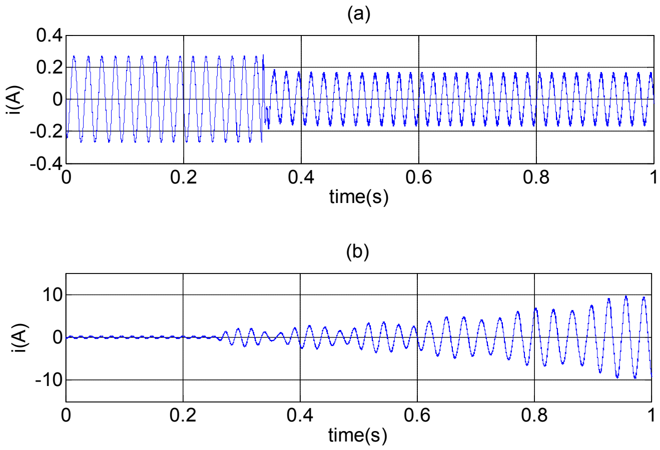

Figure 5. Simulation verification result when the rotation speed is 50Hz. (a) current vibration of AMB control system with compensation angle $\theta_k = \pi$. (b) current vibration of AMB control system with compensation angle $\theta_k = 0$.

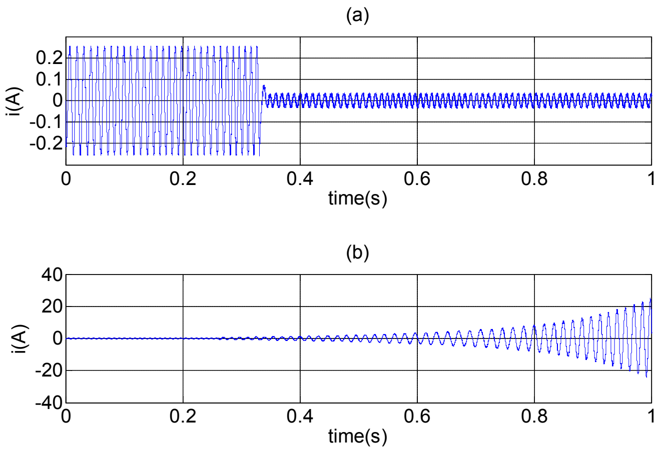

Figure 6. Simulation verification result when the rotation speed is 100Hz. (a) current vibration of AMB control system with compensation angle $\theta_k = \pi / 2$. (b) current vibration of AMB control system with compensation angle $\theta_k = 0$.

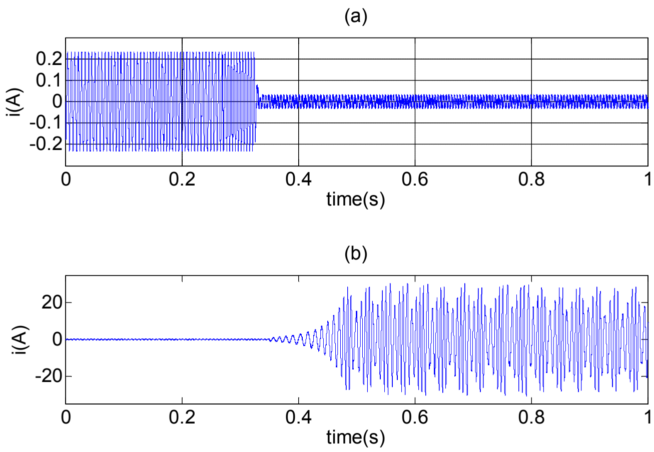

Figure 7. Simulation verification result when the rotation speed is 200Hz. (a) current vibration of AMB control system with compensation angle $\theta_k = 0$. (b) current vibration of AMB control system with compensation angle $\theta_k = \pi / 2$.

B. Simulation result comparison

Many previous researches on vibration force suppression is mainly about to suppress the current stiffness component of vibration force, which can not eliminate the synchronous force completely for the reason that the synchronous force contains not only synchronous current but also vibration displacement.

The convergence rates and effect of the proposed method and previous method which only suppress the synchronous current component were compared. The parameters were suitable selected and the simulation conducted at the rotation speed of 12000rpm (200Hz). Before 0.2s, the control strategies were scatter PID. Time ranges from 0.2s to 0.5s, conventional algorithm of current suppression was proposed. In 0.5s, The SRF-based method was switched into the AMB control system, and after 0.5s, the proposed method become effective.

As shown in Fig. 8, compared with method without displacement stiffness suppression, obviously, the amplitude of the synchronous vibration force signal after the implementation the proposed method is smaller. The control current can be minimized in amplitude within 0.1s.

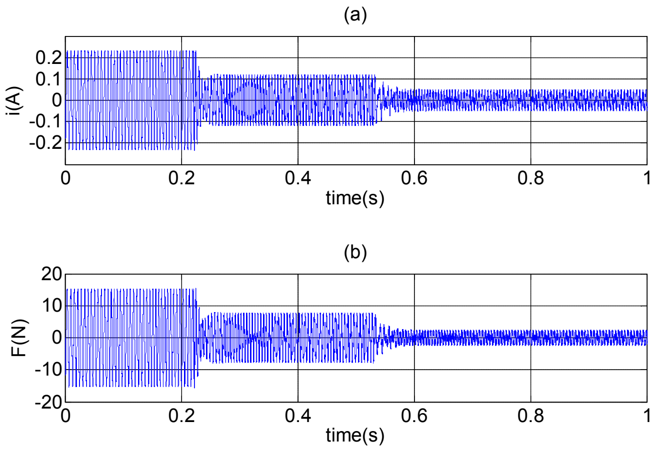

Figure 8.Comparison of suppression effect between the method with current suppression only and the novel SRF- based method at 12000r/min. (a) control current after two method applied. (b) vibration force after two method applied.

VI. Conclusion

In this paper, a novel method for direct vibration force control based on SRF has been applied. Since the vibration force was directly set as the control target. Compared with conventional method for vibration force suppression, the strategy proposed has a batter suppression effect and dynamic performance. Meanwhile, the SRF–based transformation method can ensure the stability of the whole close-loop system by only adjusting one parameter which is compensation angle and the simple structure of proposed method make it more convenient to implement. Simulation results demonstrate that this method can attenuate synchronous vibration force of magnetic suspended rotor system at different rotational speed effectively.

REFERENCES

[1] S. Q. Zheng, J. J. Sun, C. X. Miao, J. C. Fang "Vibration suppression control for AMB-supported motor driveline system using synchronous rotating frame transformation," *IEEE Transactions on Industrial Electronics*, vol. 62, no. 9, pp. 5700-5708, 2015.

[2] J. Karttunen, S. Kallio, P. Peltoniemi, P. Silventoinen " Decoupled vector control scheme for dual three-phase permanent magnet synchronous machines" *IEEE Trans. Ind. Electron*, vol. 61, no. 5, pp. 2185-2196,May 2014.

[3] H. Ohno, "Bridging semiconductor and magnetism," *Journal of Applied Physics*, vol. 113, no. 13, pp. 136509, 2013.

[4] J Shi ,R Zmood, LJ Qin "The Direct Method for Adaptive Feed-Forward Vibration Control of Magnetic Bearing Systems,"*Seventh International Conference on Control, Automation, Robotic and Vision,* Singapore 2002.

[5] C. Bi, D. Z. Wu, Q. Qi, "Automatic learning control for unbalance compensation in active magnetic bearings," *IEEE Transactions onMagnetics*, vol. 41, no. 7, pp. 2270-2280,2015.

[6] R. Herzog, P. B¨uhler, and C. G¨ahler "Unbalance compensation using generalized notch filters in the multivariable feedback of magnetic bearings," *IEEE Transactions onControl Systems Technology*, vol.45, no.5, pp. 580-586,1996.

[7] H. Gao, L. Xu, and Y. Zhu "Compensation control of real-time unbalance force for active magnetic bearing system,"*Trans. Nanjing Univ. Aeronautics Astrosp* vol.28, no.2, pp. 183-191,2011.

[8] P. L. Cui, G. Z. Zhao, J. C. Fang, H. T. Li "Adaptive control of unbalance vibration for magnetic bearings based on phase-shift notch filter within the whole frequency range," *Journal of Vibration & Shock* .2015.

[9] K. Zhang, S. Q. Zheng, and J. Yang. "Harmonic Disturbance Suppression for Magnetic Bearing System Based on Synchronous Rotating Frame Transformation." *Chinese control conference* pp. 4998-5003,2017.

[10] K. Y. Lum, V. T. Coppola, and D. S. Bernstein, "Adaptive autocentering control for an active magnetic bearing supporting rotor with unknown mass imbalance," *IEEE Trans.Control Syst. Technol.*, vol.4 no.5, pp. 587-597,1996.

[11] Q. Chen, G. Liu, B. C. Han, "Unbalance vibration suppression for AMBs system using adaptive notch filter,"*Mechanical Systems & Signal Processing* ., vol.93 , pp. 136-150,2017.